Silencing of end-joining repair for efficient site-specific gene insertion after TALEN/CRISPR mutagenesis in *Aedes aegypti*

Sanjay Basu[a,1], Azadeh Aryan[a,1], Justin M. Overcash[a], Glady Hazitha Samuel[a], Michelle A. E. Anderson[a], Timothy J. Dahlem[b], Kevin M. Myles[a,2], and Zach N. Adelman[a,2]

[a]Fralin Life Science Institute and Department of Entomology, Virginia Tech, Blacksburg, VA 24061; and [b]Mutation Generation and Detection Core, Health Science Center Core Research Facility, University of Utah, Salt Lake City, UT 84132

Edited by Anthony A. James, University of California, Irvine, CA, and approved February 24, 2015 (received for review February 6, 2015)

Conventional control strategies for mosquito-borne pathogens such as malaria and dengue are now being complemented by the development of transgenic mosquito strains reprogrammed to generate beneficial phenotypes such as conditional sterility or pathogen resistance. The widespread success of site-specific nucleases such as transcription activator-like effector nucleases (TALENs) and clustered regularly interspaced short palindromic repeats (CRISPR)/Cas9 in model organisms also suggests that reprogrammable gene drive systems based on these nucleases may be capable of spreading such beneficial phenotypes in wild mosquito populations. Using the mosquito *Aedes aegypti*, we determined that mutations in the FokI domain used in TALENs to generate obligate heterodimeric complexes substantially and significantly reduce gene editing rates. We found that CRISPR/Cas9-based editing in the mosquito *Ae. aegypti* is also highly variable, with the majority of guide RNAs unable to generate detectable editing. By first evaluating candidate guide RNAs using a transient embryo assay, we were able to rapidly identify highly effective guide RNAs; focusing germ line-based experiments only on this cohort resulted in consistently high editing rates of 24–90%. Microinjection of double-stranded RNAs targeting *ku70* or *lig4*, both essential components of the end-joining response, increased recombination-based repair in early embryos as determined by plasmid-based reporters. RNAi-based suppression of Ku70 concurrent with embryonic microinjection of site-specific nucleases yielded consistent gene insertion frequencies of 2–3%, similar to traditional transposon- or ΦC31-based integration methods but without the requirement for an initial docking step. These studies should greatly accelerate investigations into mosquito biology, streamline development of transgenic strains for field releases, and simplify the evaluation of novel Cas9-based gene drive systems.

Aedes | CRISPR | TALEN | transgenic | recombination

Mosquitoes transmit disease agents that cause malaria, dengue fever, chikungunya, and more. Conventional control strategies based on insecticides, bed nets, source reduction, vaccines, and drug treatments are now being complemented by transgenic approaches, which may soon include pathogen-resistant mosquito strains. Although development of these strategies is ongoing, field releases of first-generation technologies have had some remarkable successes (1, 2). Significant effort is currently being expended to develop transgene-based approaches with so-called "gene drive" systems designed to increase the incidence of inheriting specific alleles in a target population (3). Although a number of theoretical systems have been proposed, only one based on the site-specific homing endonuclease I-SceI has been shown to successfully drive a genetic modification into a mosquito population in large cage studies (4).

Unlike homing endonucleases, which are difficult to re-engineer, site-specific nucleases based on the type II clustered regularly interspaced short palindromic repeats (CRISPR)/Cas9 are unrivaled in the ease with which they can be tailored to a wide range of potential target sequences, already leading to the proposal of alternative gene drive designs and regulatory structure based on these more facile genetic tools (5, 6). Identified in type II *Streptococcus pyogenes* as a heritable immune defense mechanism against viruses and plasmids (7), endogenous CRISPR loci are comprised of 30–40 nucleotide (nt) variable sequences separated by short direct repeats. CRISPR locus transcripts are used to generate short CRISPR RNAs (crRNAs) that act in conjunction with a common transactivating-RNA (trRNA) to guide Cas9 endonuclease to the complementary double-stranded DNA (dsDNA) target site. An advancement in this technique has led to coupling of the crRNA and trRNA into a single chimeric guide RNA (8), resulting in a two-component system to cleave an 18- to 20-nt target sequence. However, the effectiveness of the CRISPR/Cas9 system in disease vector mosquitoes has not yet been evaluated.

Transcription activator-like effector nucleases (TALENs) are also a two-component site-specific nuclease system and have been used in genomic editing of a number of different genomes including the mosquitoes *Ae. aegypti* (9) and *Anopheles gambiae* (10). TALENs are hybrid proteins consisting of a TAL DNA binding domain (discovered in the plant pathogenic bacteria *Xanthomonas*) and the FokI nuclease domain (11). An individual TALEN consists of a left and right monomer protein, each with its own FokI nuclease domain that, on dimerization, induces

Significance

Mosquitoes are vectors of both parasites and viruses responsible for high-impact diseases including malaria, dengue, and chikungunya. Novel interventions based on genetic modification of the mosquito genome are currently being developed and implemented. To comprehensively exploit such interventions, detailed knowledge of mosquito physiology, genetics, and genome engineering are required. We developed and validated a two-step process for performing high-efficiency site-specific insertion of genetic material into the mosquito genome by first evaluating candidate site-specific nucleases in a rapid format, followed by germ line-based editing where the choice of DNA repair response is constrained. This model should significantly accelerate both basic and applied research concerning disease vector mosquitoes.

Author contributions: S.B., A.A., J.M.O., G.H.S., T.J.D., K.M.M., and Z.N.A. designed research; S.B., A.A., J.M.O., G.H.S., and M.A.E.A. performed research; T.J.D. contributed new reagents/analytic tools; S.B., A.A., J.M.O., G.H.S., M.A.E.A., T.J.D., K.M.M., and Z.N.A. analyzed data; and S.B., A.A., T.J.D., K.M.M., and Z.N.A. wrote the paper.

The authors declare no conflict of interest.

This article is a PNAS Direct Submission.

[1]S.B. and A.A. contributed equally to this work.

[2]To whom correspondence may be addressed. Email: mylesk@vt.edu or zachadel@vt.edu.

This article contains supporting information online at www.pnas.org/lookup/suppl/doi:10.1073/pnas.1502370112/-/DCSupplemental.

Downloaded by guest on January 16, 2021

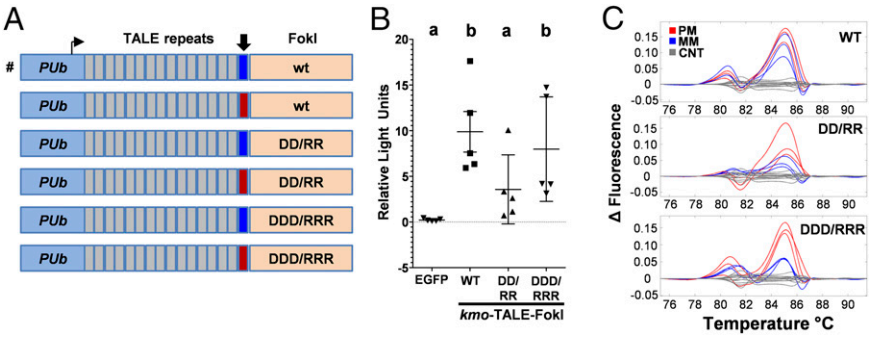

Fig. 1. Heterodimeric TALEN activity in mosquito embryos. (*A*) Representation of the TALEN constructs used to target *Ae. aegypti kmo*. All possessed the same set of TALE repeats with the exception of the final 1/2 repeat, which either perfect-matched (red) or was mismatched (blue) to the target site (block arrow). Constructs also differed in the FokI domain as indicated. Architecture used in ref. 9 is indicated (#). (*B*) SSA assay to detect TALEN activity in mosquito embryos. Each point represents a group of ∼100 injected embryos; mean and SD are indicated. Groups were found to be significantly different by ANOVA ($P < 0.05$), with assignment to groups (a, b) by Dunnett's multiple comparison test. (*C*) HRMA-based analysis of amplicons obtained from mosquito embryo DNA 24 h following injection with the indicated *kmo* TALEN pair [MM (mismatched) and PM (perfect match)] or from noninjected controls (CNT).

dsDNA breaks. Initially, WT versions of the FokI domain were used in TALEN architectures; however, activity at off-target sites was attributed to the homodimerization of left or right TALEN monomers (left-left or right-right) (12). Targeted mutations of the FokI dimerization plane, R487D (FokI-DD) or D483R (FokI-RR), established a requirement for heterodimerization of the TALEN left and right protein monomers that significantly reduced off-target activity (13, 14). However, these improvements also decreased target activity by reducing dimerization energy (15). Introduction of secondary mutations that added oppositely charged amino acids to each version, R487D and N496D (FokI-DDD) or D483R and H537R (FokI-RRR), restored activity to near WT levels while still maintaining decreased off-target activity (15). The efficacy of each of the different TALEN architectures (WT vs. DD/RR vs. DDD/RRR) has not yet been investigated in either *Ae. aegypti* or *An. gambiae.*

Early attempts at generating transgenic mosquitoes using transposon-based systems resulted in some rare successes (16–18), but efficient methods of mosquito transformation were not developed until almost 10 years later (19, 20), ushering in the current era of mosquito genome manipulation. This technology has led to the generation of mosquito strains with pathogen-resistant (21–23), conditional sterile (24, 25), flightless (26), and sex-biased (27) phenotypes. Similarly, rare successes have been reported for homology-directed repair (HDR) of nuclease-induced double-stranded DNA breaks (DSBs) using an exogenous donor template, documented in both the dengue vector, *Ae. aegypti* (28, 29), and the malaria vector, *An. gambiae* (30), but at rates less than 0.1%. Although site-specific nucleases may increase both the ease and efficiency with which DSBs can be introduced into the mosquito genome, the fact that both nonhomologous end-joining (NHEJ) and HDR are in competition for access to the break site, with NHEJ predominating (31, 32), represents a major bottleneck in efforts to re-engineer the mosquito genome for purposes of disease control.

Loss of NHEJ components such as Lig4 in *Drosophila melanogaster* (33) or Ku70 in *Bombyx mori* (34) exhibits significant increases in HDR, suggesting that similar results may be obtained by targeting the homologous genes in mosquito species. Here we describe a two-step process for site-specific gene editing of *Ae. aegypti* mediated by TALEN or CRISPR/Cas9 nucleases. We observed substantial variability in the effectiveness of engineered nucleases to induce detectable lesions at their target sites both within and between target genes. Evaluating a large pool of synthetic guide RNAs (sgRNAs) for each gene streamlined downstream steps and yielded consistent germ-line editing rates of 24–90%. Combining site-specific nucleases with RNAi-based suppression of components of the NHEJ response substantially improved rates of homology-directed repair, with rates on par with transposon- or ΦC31-based integration methods but without the requirement for an initial docking step. As with the development of initial transgenic technology, this two-step HDR approach should dramatically accelerate efforts to engineer mosquito genomes for genetic control strategies, as well as enable investigations into the basic biology of important vector species.

Results

Although TALEN-mediated gene editing has been demonstrated in mosquitoes (9, 10), the influence of different TALEN architectures on the induction of DSBs has not been examined. We generated six TALEN pairs, targeting genes related to mosquito immunity (*dcr2*, *ago2*) or DSB repair (*lig4*) pathways. However, following injection of embryos, we failed to recover any heritable gene editing events (*dcr2, ago2*; Table S1) or evidence of nuclease activity in transient embryos assays (*dcr2, ago2, lig4*). As the architecture of these TALENs use an obligate heterodimeric FokI nuclease domain and a matching final half-repeat, we sought to determine the effect of these changes on TALEN activity. The previously reported TALEN, *kmo-exon5* (9), which targets the kynurenine 3-monoxygenase (*kmo*) gene critical for eye pigmentation, was modified to contain either a perfectly matching or mismatched final half-TALE repeat, in combination with a homodimeric WT or heterodimeric DD/RR or DDD/RRR mutant FokI domain (Fig. 1*A*). The activity of these modified TALENs was determined in transient embryonic assays using either a single-strand annealing (SSA)-based reporter (35) or high-resolution melt analysis (HRMA) (36). For the SSA reporter assay, dsDNA break induction is proportional to the restoration of a luciferase ORF on repair via the SSA pathway. For HRMA, an amplicon derived from a mixed population of WT and mutant sequences will melt at a different temperature than a uniform amplicon. In the presence of a fluorescent dye that binds only to dsDNA, these nonuniform melt profiles cause a change in fluorescence that is proportional to the abundance of mutant sequences in the starting amplicon (the presence of SNPs, indels, etc., are potentially confounding and HRMA assays should avoid such regions). In each case, the activity of TALENs containing a DD/RR FokI was significantly lower than those with a WT or DDD/RRR mutation (Fig. 1 *B* and *C*), consistent with previous findings in *Drosophila* (37). In the presence of a matching final repeat, DDD/RRR TALENs had similar activity as those with the WT domain. However, in the presence of a mismatched final 1/2 repeat, the presence of the DDD/RRR mutation reduced TALEN activity (Fig. 1*C*).

To determine the effect on germ-line editing rates, a *kmo-exon5* TALEN with DDD/RRR FokI domains was injected into *Ae. aegypti* embryos, and heritable mutations were identified via failure to complement an existing mutation (kh^w) in the same target gene (AAEL008879) (9). The presence of a DDD/RRR FokI domain reduced germ-line editing to 16% (Table S1), which is about half of the rate obtained with the WT domain (9). Thus, when TALEN binding is robust, the effect of the DDD/

GENETICS

Downloaded by guest on January 16, 2021

RRR mutation on editing efficiency appears to be small, but if TALEN binding is weakened (in this case through the mismatched position), then the DDD/RRR mutations have a larger influence on the editing rate. With this in mind, six TALENs were reassembled to contain a WT FokI domain. With two of the six TALEN pairs (*lig4*-A, *lig4*-B), we were still unable to detect gene editing by HRMA. However, the presence of the WT domain in the remaining four TALEN pairs resulted in a substantial increase in gene editing, both in transient embryo assays (Fig. S1) and in germ-line experiments for the TALEN targeting *dcr2*-exon5 (Table S1). This indicates that the architecture of the FokI domain influences the rate of TALEN cleavage at target sites in the mosquito genome.

Given the substantially lower cost and ease of use of the CRISPR/Cas9 gene editing system (38), we developed a series of short guide RNAs targeting the *Ae. aegypti kmo* gene (Fig. S2*A*). Following injection of purified Cas9 protein, crRNA, and trRNA that target two overlapping sites within the previously validated TALEN target site (*kmo*-exon5), we readily observed gene editing by HRMA (Fig. S2*B*). Subsequent experiments demonstrated that a single fused sgRNA was more effective at editing an identical target sequence than the crRNA + trRNA combination (Fig. S2*C*). Targeting six other sequences in the same exon revealed substantial variability in sgRNA-directed editing, with three sgRNAs exhibiting higher levels of editing (Δ fluorescence > 0.15), two sgRNAs exhibiting lower editing rates (Δ fluorescence = 0.04–0.015), and one indistinguishable from those of the control (Fig. S2 *D* and *E*). Similar results were obtained when substituting Cas9 mRNA for purified protein, although editing rates were generally higher with the latter (Fig. S3).

Although the CRISPR/Cas9 system was clearly effective in *Ae. aegypti*, we considered that editing rates may vary across the genome. Therefore, we designed more than 40 additional sgRNAs targeting five different genes (*loqs*, *r2d2*, *ku70*, *lig4*, and *nix*) and evaluated their editing potential in transient embryo assays using HRMA (*SI Appendix*). Effective sgRNAs (Δ fluorescence > 0.05) were identified for each of the targeted genes, but success rates varied widely (range, 10–70%) on a gene-to-gene basis (Table 1). When compared, highly active sgRNAs did not reveal any consensus (Fig. S4), nor did they conform to previously published design criteria (39). The most effective sgRNAs for each target gene were subsequently used in germ-line experiments to determine rates of heritable mutations. In all cases, sgRNAs that were previously validated in transient embryo assays induced heritable mutations at high frequency (24–90%; Table 2). In the case of *kmo*, somatic activity was readily observed (Fig. 2 *A–D*), with both insertions and deletions detected at the target site (Fig. 2*E*). Even in the absence of a visible phenotypic marker, mutations in the other target genes were easily detected in pooled G_1 progeny using HRMA (Fig. S5). Thus, we conclude that the CRISPR/Cas9 system is highly efficient at editing the genome of *Ae. aegypti*, and prescreening candidate sgRNAs in transient embryo assays consistently identified highly functional nucleases.

Table 1. Effectiveness of sgRNAs between and within genes

Vectorbase ID	Gene	No. sgRNAs	HRMA^{+}	HMRA^{++} (>0.05)
AAEL008879	*kmo*	8	7	5
AAEL017365	*lig4*	10	2	1
None	*ku70*	4	3	1
AAEL008687	*loqs*	12	11	3
AAEL011753	*r2d2*	10	6	1
None	*nix*	8	4	2
Total		52	33 (63%)	13 (25%)

Table 2. CRISPR mutagenesis is highly efficient in *Ae. aegypti*

Target	sgRNA	No. injected	Total G_0	Fertile G_0	Mutant G_1[†]
kmo	519*	830	170 (20.5%)	84 (49.4%)	27/85 (32.1%)
lig4	#7	1,110	176 (15.8%)	ND	8/23 (34.8%)
ku70	#3	613	172 (28%)	77 (44.8%)	10/42 (23.8%)
r2d2	#6	565	121 (21.4%)	51 (42.1%)	20/33 (60.6%)
loqs	#3	548	124 (22.6)	62 (50%)	27/30 (90.0%)

ND, not determined.

[†]Number of G_0 individuals that produced mutant progeny/total.

Previous studies that examined the promiscuity of the CRIPSR-Cas9 system have found evidence of a seed sequence of 8–12 bp largely responsible for DNA binding (38). Single mismatches between sgRNA and the target site within this region significantly decrease the likelihood of DNA cleavage, whereas those with a conserved seed sequence and protospacer adjacent motif site (NGG) may be subject to off-target dsDNA breaks. Using the flyCRISPR target finder (40), we identified the most likely potential off-target sites in the mosquito genome for four highly active sgRNAs and analyzed them using HRMA. No evidence of off-target cleavage events could be identified (Fig. S6).

The generation of loss-of-function mutant organisms necessitates genotyping of individuals from successive generations, both for propagation and experimentation. Although feasible for a small number of strains, this becomes increasingly onerous as the number of strains increases. Multiple groups have reported the ability to insert exogenous sequences at specific sites in the mosquito genome to facilitate both the maintenance and identification of mutant stock strains (28–30). However, in none of these cases was the efficiency of the homologous recombination sufficient for routine use. We hypothesized that loss of components of the NHEJ pathway would increase the frequency of repair by the *Ae. aegypti* HDR pathway (33), thereby increasing the efficiency of gene insertion into TALEN- or CRISPR-induced DSBs in the mosquito. Unfortunately, *lig4* mutant alleles were quickly lost from our colonies (Fig. S7), suggesting that *Ae. aegypti* may not be able to tolerate complete loss of NHEJ. Thus, for our experiments, we used RNAi to temporarily suppress NHEJ activity in the early embryo. Mosquito embryos were injected with reporter constructs for monitoring either the SSA (a proxy for HDR; Fig. 3*A*) or NHEJ DSB repair pathways (Fig. 3*B*), along with dsRNA corresponding to either EGFP (control) or NHEJ components *lig4* or *ku70*; DSB induction was mediated by the homing endonuclease Y2-I-AniI (35). As expected, knockdown of NHEJ components increased recombination-based repair (Fig. 3*C*). However, depleting Ku70 decreased the rate of NHEJ-based repair, whereas diminished Lig4 increased both SSA and NHEJ activity (Fig. 3*D*). Similar effects were observed with a second dsRNA molecule targeting *ku70* or by targeting *ku80* (Fig. S8).

To determine the effect of knocking down *ku70* on HDR-based insertion of a transgene in the germ line, embryos were injected with either the *kmo-exon5* or *dcr2-exon5* TALENs, a donor vector, and either no dsRNA or dsRNA targeting EGFP or *ku70* (Fig. 4*A*). The donor vector consisted of the *PUb*-EGFP reporter and 1–2 kb of flanking sequence homologous to the respective target sites. EGFP^{+} progeny were recovered from all experiments where *ku70* dsRNA was present but not from experiments with the same TALENs/donors when no dsRNA or EGFP dsRNA was included in the injection mix (Table 3) in a manner that was highly significant (Fisher's exact test, P = 0.0119). EGFP fluorescence in transgenic larvae was easily observed (Fig. 4*B*). Precise insertion of the *PUb*-EGFP cassette at the TALEN target sites was confirmed with PCR (Fig. 4*C*). The minimum rate of gene knockin over three separate experiments

Downloaded by guest on January 16, 2021

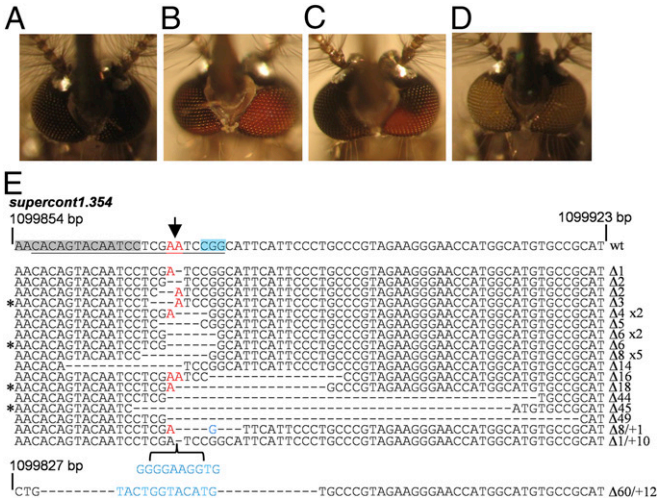

Fig. 2. Somatic and germ-line CRISPR/Cas9 editing of *Ae. aegypti*. White-light photographs of WT eyes (*A*), G_0 individuals showing somatic CRISPR-editing (*B* and *C*), and germ line-based CRISPR-edited in G_1 progeny (*D*). (*E*) Analysis of indels in CRISPR-edited progeny. Top line represents WT sequence; subsequent lines show individual mutant sequences. Underlined text indicates the crRNA target sequence including the PAM (highlighted in blue) and cleavage point (red letters and black arrow); the *kmo*-exon5 TALEN spacer site is shown for comparison (gray). Deleted bases are denoted by dashes and inserted bases are shown in blue. The number of deleted (Δ) or inserted (+) bases and their occurrence are indicated to the right; in-frame mutations are indicated (*) to the left.

was ~2.3%, similar to the average transformation efficiency in this species using conventional transposon-based or ΦC31-based integration methods. To determine whether similar benefits in HDR-based integration of a transgene could be obtained using the CRISPR/Cas9 system, we reinjected the KMO-*PUb*-EGFP donor construct with Cas9 mRNA, sgRNA519*, and *ku70* dsRNA. From 1,880 injected embryos, 285 survived to adulthood and 95 were fertile. Of these, two independent founders produced $EGFP^+$ progeny, a transformation rate of 2.1%. We conclude that efficient HDR-based integration of transgenic constructs is possible using TALEN or CRISPR-based nucleases.

Discussion

Over the last 20 years, control strategies based on manipulating the genomes of insect vectors have progressed from theoretical to full-scale releases. Technologies used thus far are based on the random integration of transposable elements into the genome; such insertions must be thoroughly characterized with respect to effects on both the fitness of the mosquito (41, 42) and the stability/expression of the transgene (43). Although some of this effort can be reduced by reusing integration sites via ΦC31 gene targeting (23, 43, 44), this still leaves a relatively small portion of the genome currently accessible to manipulation, namely those few regions that have accepted a transposon integration and have been determined to have few undesired effects. Manipulations are also limited by the necessity to add noncoding sequences such as promoters as part of one or more expression cassettes. Even when endogenous promoters are used, a new chromosomal context may strongly influence its ability to express the transgene. The ability to harness CRISPR/Cas9-mediated site-specific editing to insert exogenous sequences, at rates equivalent to transposon-based or ΦC31-based integration (23, 44, 45), dramatically alters the landscape for genome modification of disease vectors. For example, immune genes may be directly reprogrammed to respond more effectively to pathogen infection; host factors critical for pathogen replication may be altered in a way that maintains function but renders them unusable to the pathogen; and pathogen resistance effector genes may be introduced under the control of endogenous promoters using additional splice acceptors and inserting into an intron. Likewise, fitness effects due to linkage of deleterious alleles to transgene insertion sites may be avoided by simply inserting foreign sequences into the identical site in two independent genetic backgrounds; heterozygosity would be maintained even for regions in strong linkage disequilibrium with the transgene insertion site.

CRISPR/Cas9-based gene drive systems have been recently proposed as part of strategies to control mosquito-borne pathogens (5). Our data support the effectiveness of editing the *Ae. aegypti* germ line with the CRISPR/Cas9 system, with rates as high as 90%. However, a CRISPR/Cas9-based gene drive system would still rely on effective homology-directed repair of the DSB where a competition exists between various DNA repair pathways. Although both Ku70 and Lig4 are thought to be essential for classical NHEJ-based repair (32), depleting these components had opposing effects on end-joining–based repair, even though SSA, a form of HDR, increased in both cases. Although RNAi-based targeting was effective in increasing HDR-based integration, we were unable to propagate *lig4* mutations for more than one to two generations, even in the heterozygous state, suggesting that NHEJ may be critical to mosquito fertility/viability. Thus, temporary suppression of NHEJ via RNAi appears to be preferable to complete inactivation for HDR experiments. A more complete understanding of how double-stranded break repair occurs in *Ae. aegypti* is needed to further advance our capability to manipulate mosquito genomes and aid the development of CRISPR/Cas9-based gene drive systems.

Targeted mutations of the dimerization plane of the WT FokI nuclease, R487D and N496D (FokI-DDD) or D483R and H537R (FokI-RRR), decrease the potential for off-target activity while maintaining on-target activity of TALENs (11, 13–15). Although the activity of TALENs with the obligate heterodimeric DDD-RRR domains was similar to those with the WT

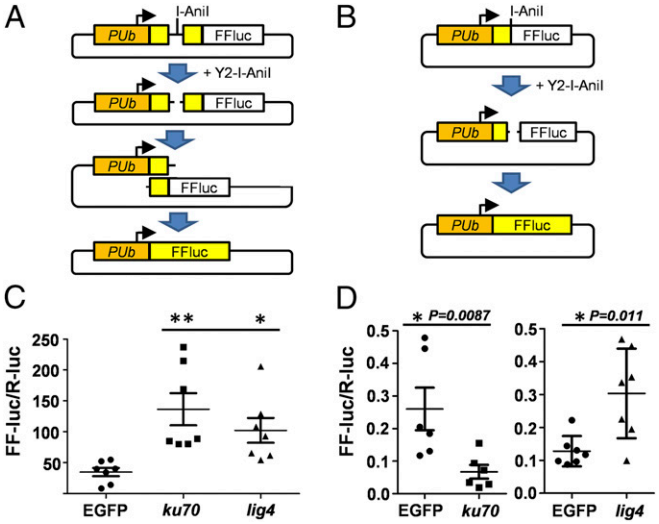

Fig. 3. Suppression of NHEJ components increases recombination activity in mosquito embryos. Representation of the plasmid constructs used to detect SSA (*A*) or NHEJ (*B*). Relative light units observed from embryos 48 h after injection with the SSA sensor (*C*) or NHEJ sensor (*D*) in the presence of the indicated dsRNA. Each point represents a pool of ~100 embryos. Data were trimmed by removing highest/lowest points from all samples (experimental and control). For *C*, statistical differences were determined by ANOVA followed by Dunnett's multiple comparison test; statistically different groups are indicated (*$P < 0.05$; **$P < 0.01$). For *D*, statistical differences were determined with a two-tailed *t* test (Mann-Whitney); *P* values are indicated.

GENETICS

Downloaded by guest on January 16, 2021

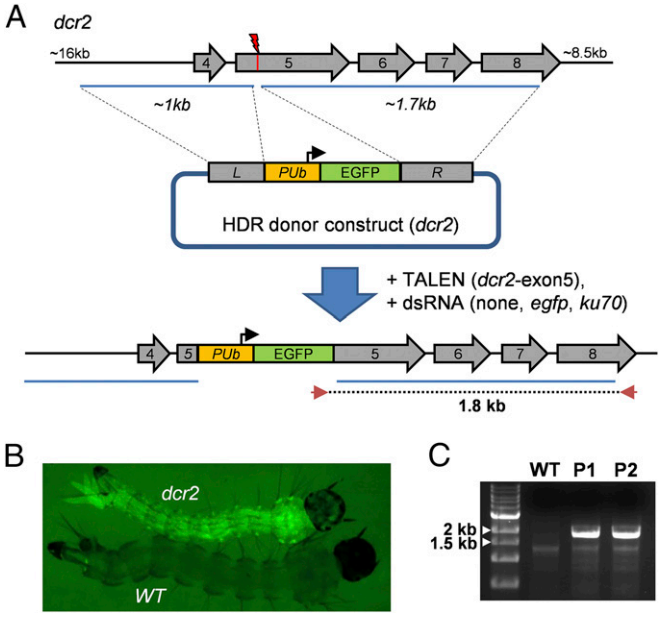

Fig. 4. Site-specific HDR-based gene insertion. (*A*) Representation of the HDR donor construct used to insert the *PUb*-EGFP expression cassette into exon5 of *dcr2*. Block arrows represent *dcr2* exons 4–8; blue bars indicate sequences used as left (L) and right (R) homology arms in the circular donor construct. TALEN target site is indicated by red vertical line; PCR primers used to confirm integration into the target site are indicated by red arrowheads. (*B*) Transgenic larvae following site-specific insertion of the *PUb*-EGFP cassette. (*C*) PCR confirmation of HDR-mediated site-specific insertion of the *PUb*-EGFP transgene.

FokI in *Drosophila* (37), we observed a substantial decrease in TALEN activity with this architecture in the mosquito *Ae. aegypti*. Thus, in scenarios where TALENs are to be used to modify the genomes of vector species, the WT FokI domain appears to be the most effective at inducing germ-line mutations and HDR events.

Although both TALENs and CRISPR/Cas9 were highly effective in generating targeted mutations, throughput was substantially higher for the CRISPR/Cas9 system. Although the majority of sgRNAs resulted in some degree of editing, we recommend that only those displaying the highest levels of activity be used in germ-line experiments. Thus, we propose a two-step approach for gene editing experiments in difficult to manipulate organisms such as mosquitoes, whereby a large cohort of sgRNAs are evaluated in vivo (in our case, early embryos), with only highly ranking candidates going forward to germ line-based experiments. Combining this two-step approach with the transient suppression of NHEJ components, such as Ku70, indicates that experiments involving the site-specific integration of transgenes into disease vector mosquitoes should be greatly accelerated.

Materials and Methods

Plasmid Construction. TALEN plasmids targeting the *Ae. aegypti kmo* gene were as previously described (46). TALEN expression plasmids targeting *dcr2*, *ago2*, and *lig4* genes were generated by the University of Utah Mutation Generation and Detection (MGD) Core using the TALEN Golden Gate kit (11), with modifications as previously described (36, 47). Briefly, TALEN target sites were designed using TALEN Effector Nucleotide Targeter 2.0 (48). Design criteria for target site selection were as follows: (*i*) spacer length of 14–18; (*ii*) TALE repeat array length of 15–21; and (*iii*) applying all additional options that restrict TALEN target site choice. The uniqueness of potential TALEN target sequences was determined by performing a BLAST analysis against the *Ae. aegypti* genome, ensuring that no highly similar left and right binding sites were in close proximity. Donor vectors for HDR-based transgene insertion were generated using standard cloning methods by inserting amplicons derived from the respective target regions upstream and downstream of the *PUb*-EGFP cassette in the previously described vector pSLfa-*PUb*-EGFP (49). TALEN target site sequences and detailed assembly methods of both TALENs and donor vectors are provided in *SI Appendix*.

Mosquitoes and Embryonic Injections. *Ae. aegypti* mosquitoes from both Liverpool (LVP) and Ub_{L40}-EGFP#P17A (49) strains were maintained in an insectary at 28 °C and 60–70% humidity, with a 14/10-h day/night light cycle. All photographs of larvae and adult mosquitoes were obtained using a Leica MZ16FL microscope with a Canon Powershot S3 IS digital camera. Embryonic injections were performed as described previously (46). For TALEN-based editing experiments, injection mixes contained 0.3 μg/μL of each TALEN expression construct. For HDR germ-line experiments, dsRNA (see *SI Appendix* for oligonucleotides and methods used for preparing dsRNA; 0.1 μg/μL) was coinjected with TALENs (0.2 μg/μL each) and the respective donor construct (0.2 μg/μL). G_0 survivors were mated with the parental strain and progeny screened for EGFP expression. SSA and NHEJ plasmid assays in mosquito early embryos were performed as previously described (46). The NHEJ plasmid assay differed from the SSA assay only in the reporter plasmid used; the Firefly luciferase ORF was interrupted by the insertion of an I-AniI recognition site (see *SI Appendix* for details). LVP embryos were injected with either SSA or NHEJ assay constructs (0.2 μg/μL), a plasmid construct coding for Y2-I-AniI homing endonuclease (0.2 μg/μL), and a normalization control plasmid (pKhsp82-Renilla) encoding Renilla luciferase (0.2 μg/μL) and snap-frozen at 48 h after injection. Embryos were homogenized, and luciferase values were determined. For CRISPR/Cas9, an injection mix was assembled containing 0.1 μg/μL of each sgRNA and the desired concentration of Cas9 mRNA or protein (and trRNA, where applicable) at 0.6 μg/μL unless otherwise stated. The injection mix with Cas9 protein was incubated at 37 °C for 20 min and then stored on ice for the duration of the injections. After 24 h, each sample (100–130 embryos) was transferred to a microcentrifuge tube and snap-frozen in liquid nitrogen.

PCR Confirmation of HR Events. To confirm that the transgene was correctly inserted into the gene of interest (*dcr2*), genomic DNA was extracted from a single male G_1 ($EGFP^+$) using the Macharey-Nagel Tissue Nucleospin Kit. Primers 5′-ttttggatccTGCATCAAAATCCTTCCAATGACGGAAAT-3′ (lowercase bases indicate added restriction site) and 5′-TTCACTGCATTCTAGTTGTGGT-TTGTCC-3′ (1,795 bp) were used to amplify the target region using Platinum Pfx polymerase (Invitrogen) (94 °C for 30 s, 35 cycles of 94 °C for 10 s, 55 °C for 30 s, and 68 °C for 2 min, and 68 °C for 10 min). The resultant amplicon was gel-purified and sequenced.

Table 3. Transgene insertion following suppression of NHEJ

Target	HR arms	dsRNA	No. injected	No. G_0 (%)	No. G_0 pools	No. G_1 screened	$EGFP^+$ (#)	Rate[†]
kmo	0.6/0.5 kb	—	1,010	109 (11%)	6	>11,000	0	<1.8%
kmo	2.2/1.7 kb	—	1,030	152 (15%)	8	>12,000	0	<1.3%
kmo	2.2/1.7 kb	*egfp*	1,130	192 (17%)	9	~33,000	0	<1.0%
kmo	2.2/1.7 kb	*ku70* #1	1,090	166 (15%)	9	~33,000	P1 (1), P3 (36)	2.4%
kmo	2.2/1.7 kb	*ku70* #2	1,035	118 (11%)	5	~16,000	P2 (8)	1.7%
dcr2	1/1.7 kb	*egfp*	1,138	237 (21%)	10	~46,000	0	<0.8%
dcr2	1/1.7 kb	*ku70* #2	1,050	144 (14%)	7	~23,000	P1 (7), P2 (2)	2.7%
Total		-/*egfp*	3,298	581 (18%)	27	~91,000	0	<0.3%
		ku70	3,175	428 (13%)	21	~72,000	5	2.3%

[†]Minimum rate of gene knockin based on 50% fertility.

Downloaded by guest on January 16, 2021

CRISPR/Cas9 Reagents. Purified Cas9 protein was obtained from PNA Bio. The lyophilized pellet was dissolved in nuclease-free water to a concentration of 2.5 μg/μL, aliquoted, and stored at −80 °C. Cas9 mRNA was generated using pRGEN-Cas9-CMV (PNA BIO). One microgram of linearized DNA was used as the template for an in vitro transcription reaction using the mMessage mMachine T7 Ultra kit (Ambion). The reaction was incubated at 37 °C for 6 h, DNase treated at 37 °C for 30 min, polyA-tailed at 37 °C for 1 h, and purified using the MEGAclear Clean-Up kit (Life Technologies). sgRNA519* and sgRNA519, crRNA, and the corresponding trRNA were obtained from PNA Bio. Lyophilized RNA was dissolved in nuclease-free water to a concentration of 1 μg/μL, aliquoted, and stored at −80 °C. Otherwise, guide RNAs were generated as described in ref. 8 using the oligonucleotides listed in *SI Appendix*.

HRMA Assays. Genomic DNA was extracted from adults or embryos using the Nucleospin Tissue kit (Macherey-Nagel). Alternatively, PCR was directly performed on adult legs using the Phire Animal Tissue Direct PCR kit (Thermo Scientific) as described previously (46). HRMA primer assays were designed to generate amplicons of 80–120 bp traversing the CRISPR/TALEN target site using the LightScanner Primer Design Software (Biofire Defense). A complete list of HRMA primers used is presented in *SI Appendix*. PCR was performed in 10-μL reactions with 2 μL genomic DNA, 4 μL 2.5× LightScanner MasterMix (Biofire Defense), 200 nM of each primer, and 2 μL nuclease-free water. Reactions were conducted within a 96-well plate and sealed with optical film before cycling in a BioRad thermal cycler (95 °C for 2 min; 40 cycles of 94 °C for 30 s, 65 °C for 30 s; 94 °C for 30 s; 25 °C for 30 s; and 4 °C hold). Thermal melt profiles were generated on a LightScanner Instrument (Biofire Defense) (60–95 °C, hold 57 °C) and analyzed using the Lightscanner Call-IT 2.0 software. Samples showing mutations using HRMA were reamplified to generate a larger amplicon that was sequenced directly; Poly Peak Parser (50) was used to identify specific indels.

ACKNOWLEDGMENTS. We thank the University of Utah Mutation Generation and Detection Core for providing TALEN constructs, as well as members of the K.M.M. and Z.N.A. laboratories for technical support. This project was supported by the National Institute for Allergy and Infectious Diseases Grants AI085091, AI099843, AI103265, and AI77726.

1. Harris AF, et al. (2011) Field performance of engineered male mosquitoes. *Nat Biotechnol* 29(11):1034–1037.
2. Hoffmann AA, et al. (2011) Successful establishment of *Wolbachia* in *Aedes* populations to suppress dengue transmission. *Nature* 476(7361):454–457.
3. Alphey L (2014) Genetic control of mosquitoes. *Annu Rev Entomol* 59:205–224.
4. Windbichler N, et al. (2011) A synthetic homing endonuclease-based gene drive system in the human malaria mosquito. *Nature* 473(7346):212–215.
5. Oye KA, et al. (2014) Biotechnology. Regulating gene drives. *Science* 345(6197): 626–628.
6. Esvelt KM, Smidler AL, Catteruccia F, Church GM (2014) Concerning RNA-guided gene drives for the alteration of wild populations [published online ahead of print July 17, 2014]. *eLife*, 10.7554/eLife.03401.
7. Terns MP, Terns RM (2011) CRISPR-based adaptive immune systems. *Curr Opin Microbiol* 14(3):321–327.
8. Bassett AR, Tibbit C, Ponting CP, Liu J-L (2013) Highly efficient targeted mutagenesis of *Drosophila* with the CRISPR/Cas9 system. *Cell Reports* 4(1):220–228.
9. Aryan A, Anderson MA, Myles KM, Adelman ZN (2013) TALEN-based gene disruption in the dengue vector *Aedes aegypti*. *PLoS ONE* 8(3):e60082.
10. Smidler AL, Terenzi O, Soichot J, Levashina EA, Marois E (2013) Targeted mutagenesis in the malaria mosquito using TALE nucleases. *PLoS ONE* 8(8):e74511.
11. Cermak T, et al. (2011) Efficient design and assembly of custom TALEN and other TAL effector-based constructs for DNA targeting. *Nucleic Acids Res* 39(12):e82.
12. Miller JC, et al. (2007) An improved zinc-finger nuclease architecture for highly specific genome editing. *Nat Biotechnol* 25(7):778–785.
13. Söllü C, et al. (2010) Autonomous zinc-finger nuclease pairs for targeted chromosomal deletion. *Nucleic Acids Res* 38(22):8269–8276.
14. Szczepek M, et al. (2007) Structure-based redesign of the dimerization interface reduces the toxicity of zinc-finger nucleases. *Nat Biotechnol* 25(7):786–793.
15. Doyon Y, et al. (2011) Enhancing zinc-finger-nuclease activity with improved obligate heterodimeric architectures. *Nat Methods* 8(1):74–79.
16. Miller LH, et al. (1987) Stable integration and expression of a bacterial gene in the mosquito *Anopheles gambiae*. *Science* 237(4816):779–781.
17. McGrane V, Carlson JO, Miller BR, Beaty BJ (1988) Microinjection of DNA into *Aedes triseriatus* ova and detection of integration. *Am J Trop Med Hyg* 39(5):502–510.
18. Morris AC, Eggleston P, Crampton JM (1989) Genetic transformation of the mosquito *Aedes aegypti* by micro-injection of DNA. *Med Vet Entomol* 3(1):1–7.
19. Coates CJ, Jasinskiene N, Miyashiro L, James AA (1998) *Mariner* transposition and transformation of the yellow fever mosquito, *Aedes aegypti*. *Proc Natl Acad Sci USA* 95(7):3748–3751.
20. Jasinskiene N, et al. (1998) Stable transformation of the yellow fever mosquito, *Aedes aegypti*, with the *Hermes* element from the housefly. *Proc Natl Acad Sci USA* 95(7): 3743–3747.
21. Corby-Harris V, et al. (2010) Activation of *Akt* signaling reduces the prevalence and intensity of malaria parasite infection and lifespan in *Anopheles stephensi* mosquitoes. *PLoS Pathog* 6(7):e1001003.
22. Kokoza V, et al. (2010) Blocking of *Plasmodium* transmission by cooperative action of Cecropin A and Defensin A in transgenic *Aedes aegypti* mosquitoes. *Proc Natl Acad Sci USA* 107(18):8111–8116.
23. Meredith JM, et al. (2011) Site-specific integration and expression of an anti-malarial gene in transgenic *Anopheles gambiae* significantly reduces *Plasmodium* infections. *PLoS ONE* 6(1):e14587.
24. Thomas DD, Donnelly CA, Wood RJ, Alphey LS (2000) Insect population control using a dominant, repressible, lethal genetic system. *Science* 287(5462):2474–2476.
25. Phuc HK, et al. (2007) Late-acting dominant lethal genetic systems and mosquito control. *BMC Biol* 5:11.
26. Fu G, et al. (2010) Female-specific flightless phenotype for mosquito control. *Proc Natl Acad Sci USA* 107(10):4550–4554.
27. Galizi R, et al. (2014) A synthetic sex ratio distortion system for the control of the human malaria mosquito. *Nat Commun* 5:3977.
28. Liesch J, Bellani LL, Vosshall LB (2013) Functional and genetic characterization of neuropeptide Y-like receptors in *Aedes aegypti*. *PLoS Negl Trop Dis* 7(10):e2486.
29. McMeniman CJ, Corfas RA, Matthews BJ, Ritchie SA, Vosshall LB (2014) Multimodal integration of carbon dioxide and other sensory cues drives mosquito attraction to humans. *Cell* 156(5):1060–1071.
30. Bernardini F, et al. (2014) Site-specific genetic engineering of the *Anopheles gambiae* Y chromosome. *Proc Natl Acad Sci USA* 111(21):7600–7605.
31. Lieber MR (2010) The mechanism of double-strand DNA break repair by the nonhomologous DNA end-joining pathway. *Annu Rev Biochem* 79:181–211.
32. Williams GJ, et al. (2014) Structural insights into NHEJ: Building up an integrated picture of the dynamic DSB repair super complex, one component and interaction at a time. *DNA Repair (Amst)* 17(0):110–120.
33. Beumer KJ, et al. (2008) Efficient gene targeting in *Drosophila* by direct embryo injection with zinc-finger nucleases. *Proc Natl Acad Sci USA* 105(50):19821–19826.
34. Ma S, et al. (2014) CRISPR/Cas9 mediated multiplex genome editing and heritable mutagenesis of *BmKu70* in *Bombyx mori*. *Sci Rep* 4:4489.
35. Aryan A, Anderson MAE, Myles KM, Adelman ZN (2013) Germline excision of transgenes in *Aedes aegypti* by homing endonucleases. *Sci Rep* 3:1603.
36. Dahlem TJ, et al. (2012) Simple methods for generating and detecting locus-specific mutations induced with TALENs in the zebrafish genome. *PLoS Genet* 8(8):e1002861.
37. Beumer KJ, et al. (2013) Comparing zinc finger nucleases and transcription activator-like effector nucleases for gene targeting in *Drosophila*. *G3* 3(10):1717–1725.
38. Doudna JA, Charpentier E (2014) Genome editing. The new frontier of genome engineering with CRISPR-Cas9. *Science* 346(6213):1258096.
39. Wang T, Wei JJ, Sabatini DM, Lander ES (2014) Genetic screens in human cells using the CRISPR-Cas9 system. *Science* 343(6166):80–84.
40. Gratz SJ, et al. (2014) Highly specific and efficient CRISPR/Cas9-catalyzed homology-directed repair in *Drosophila*. *Genetics* 196(4):961–971.
41. Amenya DA, et al. (2010) Comparative fitness assessment of *Anopheles stephensi* transgenic lines receptive to site-specific integration. *Insect Mol Biol* 19(2):263–269.
42. Paton D, Underhill A, Meredith J, Eggleston P, Tripet F (2013) Contrasted Fitness Costs of Docking and Antibacterial Constructs in the EE and EVida3 Strains Validates Two-Phase Anopheles gambiae Genetic Transformation System. *PLoS ONE* 8(6):e67364.
43. Isaacs AT, et al. (2012) Transgenic *Anopheles stephensi* coexpressing single-chain antibodies resist *Plasmodium falciparum* development. *Proc Natl Acad Sci USA* 109(28):E1922–E1930.
44. Nimmo DD, Alphey L, Meredith JM, Eggleston P (2006) High efficiency site-specific genetic engineering of the mosquito genome. *Insect Mol Biol* 15(2):129–136.
45. Labbé GM, Nimmo DD, Alphey L (2010) piggybac- and PhiC31-mediated genetic transformation of the Asian tiger mosquito, *Aedes albopictus* (Skuse). *PLoS Negl Trop Dis* 4(8):e788.
46. Aryan A, Myles KM, Adelman ZN (2014) Targeted genome editing in *Aedes aegypti* using TALENs. *Methods* 69(1):38–45.
47. Hu R, Wallace J, Dahlem TJ, Grunwald DJ, O'Connell RM (2013) Targeting human microRNA genes using engineered Tal-effector nucleases (TALENs). *PLoS ONE* 8(5): e63074.
48. Doyle EL, et al. (2012) TAL Effector-Nucleotide Targeter (TALE-NT) 2.0: Tools for TAL effector design and target prediction. *Nucleic Acids Res* 40(web server issue):W117–W122.
49. Anderson MA, Gross TL, Myles KM, Adelman ZN (2010) Validation of novel promoter sequences derived from two endogenous ubiquitin genes in transgenic *Aedes aegypti*. *Insect Mol Biol* 19(4):441–449.
50. Hill JT, et al. (2014) Poly peak parser: Method and software for identification of unknown indels using sanger sequencing of polymerase chain reaction products. *Dev Dyn* 243(12):1632–1636.

GENETICS

Downloaded by guest on January 16, 2021